Received: 10 March 2020 | Revised: 6 August 2020 | Accepted: 11 October 2020
DOI: 10.1002/acs.3193

RESEARCH ARTICLE

WILEY

Adaptive output-feedback stabilization in prescribed time for nonlinear systems with unknown parameters coupled with unmeasured states

Prashanth Krishnamurthy[1] | **Farshad Khorrami**[1] | **Miroslav Krstic**[2]

[1]Control/Robotics Research Laboratory, Department of ECE, NYU Tandon School of Engineering, Brooklyn, New York,

[2]Department of Mechanical and Aerospace Engineering, University of California, San Diego, La Jolla, California,

Correspondence
Farshad Khorrami, Control/Robotics Research Laboratory, Department of ECE, NYU Tandon School of Engineering, Brooklyn, NY, USA.
Email: khorrami@nyu.edu

Summary
The prescribed-time output-feedback stabilization (ie, regulation of the state and control input to zero within a "prescribed" time picked by the control designer irrespective of the initial state) of a general class of uncertain nonlinear strict-feedback-like systems is considered. Unlike prior results, the class of systems considered in this article allows crossproducts of unknown parameters (without any required magnitude bounds on unknown parameters) and unmeasured state variables in uncertain state-dependent nonlinear functions throughout the system dynamics. We show that prescribed-time output-feedback stabilization (ie, both prescribed-time state estimation and prescribed-time regulation) is achieved through a novel output-feedback control design involving specially designed dynamics of an adaptation state variable and a high-gain scaling parameter in combination with a temporal transformation and a dual high-gain scaling based observer and controller design. While standard dynamic adaptation techniques cannot be applied due to crossproducts of unknown parameters and unmeasured states, we show that instead, the dynamics of the high-gain scaling parameter and adaptation parameter can be designed with temporal forcing terms to ensure that unknown parameters in system dynamics are dominated by a particular fractional power of the high-gain scaling parameter and the adaptation parameter after a subinterval (of unknown length) of the prescribed time interval. We show that the control law can be designed such that the system state and input are regulated to zero in the remaining subinterval of the prescribed time interval.

KEYWORDS
adaptive control, nonlinear uncertain systems, output-feedback, prescribed time, stabilization

1 | INTRODUCTION

Unlike asymptotic stabilization (ie, as time goes to ∞) which is typically addressed in most control design approaches,[2-5] "finite-time" stabilization[6-17] addresses control designs to achieve desired properties (eg, convergence to origin) within a finite time interval. Fast finite-time stabilization has been addressed in References 15,18-20 focusing on high-order

An earlier version[1] of this article was presented at the 2019 IEEE Conference on Decision and Control, Nice, France, December 2019.

uncertain nonlinear systems that can feature various fractional powers of state variables in the system dynamics and including appended dynamics with unmeasured state in References 19,20. In addition, methods to adjust the finite convergent time by appropriately picking parameters in the designed controllers are developed in References 15,18-20 to attain fast convergence (as a function of the initial conditions). "Fixed-time" stabilization[13,21-25] further requires that this finite terminal time should be bounded by a constant independent of the initial conditions. Further requiring that this fixed terminal time should be possible to be arbitrarily picked (ie, *prescribed*) by the designer yields the stronger notion of "prescribed-time" stabilization,[26-35] that is, prescribed-time stabilization requires that the convergence not just be over a finite time interval, but that the length of the time interval be a parameter that can be arbitrarily prescribed by the control designer independent of initial condition and system dynamics. This prescribed-time stabilization notion can be viewed in the physical context of controls applications such as autonomous vehicle rendezvous, missile guidance, and so on, wherein the state convergence control objective is inherently formulated over a time horizon of predefined length. Mathematically, the attaining of prescribed-time stabilization independent of initial conditions is fundamentally through the use of control gains that go to infinity as the time t approaches the prescribed terminal time T, while however ensuring that the state and control input remain bounded (and, in fact, typically not just remain bounded but actually converge to zero). The use of control gains that grow unbounded as $t \to T$ can be traced back to early work on optimal control over time intervals[36] and time base generators.[37]

Prescribed-time stabilization of a chain of integrators with uncertainties matched with the control input (ie, normal form) was addressed in References 26,27,33 based on scaling the system state by a function of time that goes to infinity as $t \to T$ and designing a controller to stabilize the system written in terms of the scaled state. A prescribed-time stabilizing controller was developed in Reference 38 for a more general class of strict-feedback-like systems based on our dual dynamic high-gain scaling based observer-controller design techniques[39-44] and introducing a set of modifications to address the prescribed-time instead of asymptotic stabilization objective in combination with a time scale transformation and a scaling parameter dynamics including time-dependent forcing terms. The state-feedback design in Reference 38 was extended to the output-feedback case in Reference 45. In this article, we consider a more general class of uncertain nonlinear strict-feedback-like systems[1] in which uncertain functions throughout the system dynamics involve combinations of unknown parameters (without requiring magnitude bounds on unknown parameters) and unmeasured state variables:

$$\begin{aligned} \dot{x}_i &= \phi_i(x,u,t) + \phi_{(i,i+1)}(x_1)x_{i+1} \quad, \ i = 1, \ldots, n-1, \\ \dot{x}_n &= \phi_n(x,u,t) + \mu_0(x_1)u, \\ y &= x_1, \end{aligned} \tag{1}$$

where $x = [x_1, \ldots, x_n]^T \in \mathcal{R}^n$ is the state, $u \in \mathcal{R}$ the input, and $y \in \mathcal{R}$ the output[2]. $\phi_{(i,i+1)}, i = 1, \ldots, n-1$, and μ_0, are known scalar real-valued continuous functions of their arguments. $\phi_i, i = 1, \ldots, n$, are scalar real-valued uncertain functions. As seen in Assumption 2 in Section 2, the functions ϕ_i that are allowed to involve parametric uncertainties (without any known magnitude bounds) coupled with unmeasured state variables and output. It is shown that while the general lines of the observer and controller designs from Reference 45 can be applied to the class of systems considered here, the presence of unknown parameters and their coupling with unmeasured states necessitate several crucial changes in the control design and stability analysis. Specifically, as discussed further in Remark 5, standard approaches to designing dynamics of adaptation parameters using augmented Lyapunov functions cannot be directly applied since the coupling between unknown parameters and unmeasured states would result in requiring that the dynamics of the adaptation parameters need to depend on the unmeasured states. While such crossproducts were addressed in Reference 46 in the context of asymptotic stabilization, the approach there relies upon analysis of asymptotic properties of the adaptation state variables and does not directly extend to the prescribed-time context. Instead, the approach proposed in this article is to consider the prescribed stabilization time interval as comprised of two subintervals (of unknown lengths) and to design the dynamic output-feedback controller based on the following strategy:

- Design the dynamics of the high-gain scaling parameter and the adaptation parameter with temporal forcing terms so as to ensure that the unknown parameters in the system dynamics are dominated by either a particular fractional power of the high-gain scaling parameter or the adaptation parameter after a subinterval (of unknown length) of the prescribed stabilization time interval.

[1]Throughout, a dot above a symbol denotes the derivative with respect to the time t as is the standard notation, for example, $\dot{x}_1 = \frac{dx_1}{dt}$.
[2]$\mathcal{R}$, $\mathcal{R}^+$, and $\mathcal{R}^k$ denote the set of real numbers, the set of nonnegative real numbers, and the set of real k-dimensional column vectors, respectively.

- Design the control law such that the system state and input are regulated to 0 in the remaining subinterval of the prescribed stabilization time interval.

To accomplish the above strategy, two additional controller state variables ($\hat{\theta}_1$ and $\hat{\theta}_2$) are introduced as adaptation parameters, the dynamics of both of which will involve temporal forcing terms. In addition, it will be seen that the dynamics of the high-gain scaling parameter (r) need to be of a significantly different form than Reference 45 and involve quadratic and fractional powers of the scaling parameter. As discussed above, the dynamics of the adaptation and scaling parameters will be constructed so as to be able to dominate the uncertain parameters in the system dynamics quickly enough (within a subinterval of the prescribed stabilization time interval) while still retaining closed-loop system stability and to enable exponential convergence of the system state and input within the remaining subinterval of the prescribed time interval. As in Reference 45, the control design utilizes a time scale transformation $\tau = a(t)$ that maps the finite time interval $[0, T)$ in terms of the original time variable t to the infinite time interval $[0, \infty)$ in terms of the new time variable τ. Thereby, by designing the controller to achieve the desired convergence properties as $\tau \to \infty$, the desired properties are effectively achieved as $t \to T$, that is, in the specified prescribed time.

The control objective and assumptions on the system (1) considered are provided in Section 2. The observer and controller designs are presented in Section 3. The main result of the article and its proof are provided in Section 4. The application of the proposed control design to an example third-order system is presented in Section 5. Concluding remarks are summarized in Section 6.

2 | CONTROL OBJECTIVE AND ASSUMPTIONS

Control objective: With $T > 0$ being a given constant (that can be picked arbitrarily by the control designer), the control objective is to design a dynamic output-feedback control law for u so that, starting from any initial condition for x, we have $x(t) \to 0$ and $u(t) \to 0$ as $t \to T$.

The assumptions imposed on the system (1) are summarized below.

Assumption 1. (*Lower boundedness away from zero of "upper diagonal" terms $\phi_{(i,i+1)}$ and μ_0*): A constant $\sigma > 0$ is known such that[3] $|\phi_{(i,i+1)}(x_1)| \geq \sigma, 1 \leq i \leq n-1$, and $|\mu_0(x_1)| \geq \sigma$ for all $x_1 \in \mathcal{R}$. Since $\phi_{(i,i+1)}$ and μ_0 are assumed to be continuous functions, this assumption can, without loss of generality, be stated as $\phi_{(i,i+1)}(x_1) \geq \sigma, 1 \leq i \leq n-1$, and $\mu_0(x_1) \geq \sigma$ with a constant $\sigma > 0$.

Assumption 2. (*Bounds on uncertain functions ϕ_i*): The functions $\phi_i, i = 1, \dots, n$, can be bounded as

$$|\phi_i(x, u, t)| \leq \theta\Gamma(x_1)\sum_{j=1}^{i}\phi_{(i,j)}(x_1)|x_j| \tag{2}$$

for all $x \in \mathcal{R}^n$ where $\Gamma(x_1)$ and $\phi_{(i,j)}(x_1), i = 1, \dots, n, j = 1, \dots, i$, are known continuous nonnegative functions and $\theta \geq 0$ is an unknown constant.

Assumption 3. (*Bidirectional cascading dominance of "upper diagonal" terms $\phi_{(i,i+1)}, i = 2, \dots, n,$*): Positive constants $\overline{\rho}_i, i = 3, \dots, n-1$, and $\underline{\rho}_i, i = 3, \dots, n-1$ are known such that $\forall x_1 \in \mathcal{R}$

$$\phi_{(i,i+1)}(x_1) \geq \overline{\rho}_i\phi_{(i-1,i)}(x_1), \quad i = 3, \dots, n-1, \tag{3}$$

$$\phi_{(i,i+1)}(x_1) \leq \underline{\rho}_i\phi_{(i-1,i)}(x_1), \quad i = 3, \dots, n-1. \tag{4}$$

Remark 1. The structure of the assumptions above is similar to Reference 45 except for the additional term θ, which is an unknown parameter (without any requirement of known magnitude bounds). It is to be noted that the structure of the bounds on uncertain functions ϕ_i in Assumption 2 allows crossproducts of unknown parameters and unmeasured state variables, which is the primary crucial challenge from an adaptive control viewpoint; the challenge is further amplified in the current context since we seek prescribed-time stabilization rather than just asymptotic stabilization.

[3]Given a vector a, the notation $|a|$ denotes its Euclidean norm. If a is a scalar, $|a|$ denotes its absolute value.

Apart from the uncertain parameter θ, the introduced assumptions are also analogous to the assumptions introduced for the dual dynamic high-gain based output-feedback control design in Reference 39, which addressed asymptotic stabilization. Assumption 1 ensures observability, controllability, and uniform relative degree (of x_1 with respect to u). Assumption 2 imposes bounds on uncertain terms in the system dynamics and essentially requires uncertain terms to be bounded linearly in unmeasured state variables with a triangular state dependence structure in the known bounds along with an uncertain parameter θ without requiring any known bounds on the uncertain parameter. While the bounds in Assumption 2 can feature multiple separate uncertain parameters θ_i, a single parameter θ is considered here for simplicity and brevity. While the upper bound in Assumption 2 could be replaced with a "lumped" upper bound $|\phi_i(x,u,t)| \leq \theta\Gamma(x_1)\sum_{j=1}^{i}|x_j|$ with a suitably redefined $\Gamma(x_1)$, the structure in Assumption 2 allows specification of more precise and tighter bounds while a lumped upper bound would be the conservative "worst-case" bound. In addition, while $\Gamma(x_1)$ could be built into the $\phi_{(i,j)}(x_1)$ functions in Assumption 2 instead of appearing separately, $\Gamma(x_1)$ is explicitly written as a separate term to allow factoring out of any common terms in the $\phi_{(i,j)}(x_1)$ functions given a particular example and therefore enable writing the $\phi_{(i,j)}(x_1)$ functions more compactly. Assumption 3 imposes constraints on the relative "sizes" (in a nonlinear function sense) of the upper diagonal terms $\phi_{(i,i+1)}$ and is vital in achieving solvability of a pair of coupled Lyapunov inequalities (Section 3.6). The functions $\phi_{(i,i+1)}$ are referred to as "upper diagonal" terms since if the dynamics (1) were to be written in the form $\dot{x} = A(x_1)x + B(x_1)u + \phi(x)$ with $\phi = [\phi_1, \ldots, \phi_n]^T$, the functions $\phi_{(i,i+1)}$ would appear on the upper diagonal of the matrix $A(x_1)$.

3 | CONTROL DESIGN

3.1 | Observer design

Since state variables $x_2, \ldots, x_n$ are not measured, we wish to design an observer to estimate these unmeasured states. In particular, we wish to design a reduced-order observer (instead of a reduced-order observer, a full-order observer can be designed instead as discussed in Remark 2). Denote the states of the reduced-order observer by $\hat{x} = [\hat{x}_2, \ldots, \hat{x}_n]^T$. Since this is a reduced-order observer, the estimate for each x_i is to be constructed as a combination of $\hat{x}_i$ and a function of x_1. In particular, the typical structure in the dynamic scaling-based observer design[39] constructs the estimate for x_i as the combination $\hat{x}_i + r^{i-1}f_i(x_1)$ where $f_i(x_1)$ are functions of x_1 that will be defined below and r is the dynamic high-gain scaling parameter whose dynamics will be designed later (Section 3.9). The dynamics chosen for r will ensure that $r(t) \geq 1$ for all time $t \geq 0$. From this structure of the estimate of x_i, it follows that the observer errors are defined as

$$e_i = \hat{x}_i + r^{i-1}f_i(x_1) - x_i\ ,\ i = 2, \ldots, n. \tag{5}$$

Per the dynamic scaling-based approach,[39] the scaled observer errors are defined as

$$\epsilon_i = \frac{e_i}{r^{i-1}}\ ,\ i = 2, \ldots, n\ ;\ \epsilon = [\epsilon_2, \ldots, \epsilon_n]^T, \tag{6}$$

that is, scaling of $e_2, \ldots, e_n$ by successive powers of r. By this definition of the scaled observer errors, it is seen that the derivative of ϵ_i will include a term given by $-(i-1)\frac{\dot{r}}{r}\epsilon_i$. In addition, since $\dot{x}_i$ includes a term given by $\phi_{(i,i+1)}(x_1)x_{i+1}$ as seen in the system dynamics (1), it can be expected that with an appropriate design of the dynamics of $\hat{x}_i$, we will have a term $\phi_{(i,i+1)}(x_1)e_{i+1}$ in $\dot{e}_i$ and hence a term $r\phi_{(i,i+1)}(x_1)\epsilon_{i+1}$ in $\dot{\epsilon}_i$ since $e_{i+1} = r^i\epsilon_{i+1}$ from (6). Therefore, it can be expected that with an appropriate design of the dynamics of $\hat{x}_i$, we should be able to obtain the dynamics of ϵ to be of the structure

$$\dot{\epsilon} = rA_o\epsilon - \frac{\dot{r}}{r}D\epsilon + \overline{\Phi} \tag{7}$$

where

- A_o is a $(n-1)\times(n-1)$ matrix with (i,j)th entry $A_{o_{(i,1)}}(x_1) = -g_{i+1}(x_1)$ for $i = 1, \ldots, n-1$, and $A_{o_{i,i+1}}(x_1) = \phi_{(i+1,i+2)}(x_1)$ for $i = 1, \ldots, n-2$.

- D is defined as [4]

$$D = \mathrm{diag}(1, 2, \ldots, n-1). \tag{8}$$

Note that D is a positive-definite matrix.

- $\overline{\Phi}$ involves the uncertain functions $\phi_1, \ldots, \phi_n$.

It is now straightforward to evaluate what the appropriate design of the dynamics of $\hat{x}_i$ should be to attain the structure of the dynamics of ϵ shown above. By simply substituting the form of e_i from (5) and the form of ϵ_i from (6), it can be seen that $\hat{x}_i$ should therefore be of the form

$$\begin{aligned}\dot{\hat{x}}_i &= \phi_{(i,i+1)}(x_1)[\hat{x}_{i+1} + r^i f_{i+1}(x_1)] - (i-1)\dot{r}r^{i-2}f_i(x_1) - r^{i-1}g_i(x_1)[\hat{x}_2 + rf_2(x_1)]\ ,\ i = 2, \ldots, n-1,\\ \dot{\hat{x}}_n &= \mu_0(x_1)u - (n-1)\dot{r}r^{n-2}f_n(x_1) - r^{n-1}g_n(x_1)[\hat{x}_2 + rf_2(x_1)],\end{aligned} \tag{9}$$

where $g_i(x_1)$ is defined as $\phi_{(1,2)}(x_1)\frac{\partial f_i(x_1)}{\partial x_1}$, or equivalently

$$f_i(x_1) = \int_0^{x_1} \frac{g_i(\pi)}{\phi_{(1,2)}(\pi)} d\pi,\ i = 2, \ldots, n. \tag{10}$$

The functions $g_i(x_1)$ will be designed based on a pair of coupled Lyapunov inequalities in Section 3.6. With the observer dynamics in (9), it can be seen by expanding the terms appearing in (7) that the term $\overline{\Phi}$ involving uncertain functions $\phi_1, \ldots, \phi_n$ is given by

$$\begin{aligned}\overline{\Phi} &= [\overline{\Phi}_2, \ldots, \overline{\Phi}_n]^T,\\ \overline{\Phi}_i &= -\frac{\phi_i(x,u,t)}{r^{i-1}} + g_i(x_1)\frac{\phi_1(x_1)}{\phi_{(1,2)}}\ ,\ i = 2, \ldots, n.\end{aligned} \tag{11}$$

Remark 2. The observer structure given in Section 3.1 is a reduced-order observer with state variables $[\hat{x}_2, \ldots, \hat{x}_n]^T$. Instead of a reduced-order observer, a full-order observer can also be used instead as in Reference 46. For this purpose, to obtain an equivalent form of the dynamics as in (7), a full-order observer can be written as

$$\begin{aligned}\dot{\hat{x}}_1 &= \phi_{(1,2)}(x_1)\hat{x}_2 - \frac{\dot{r}}{r}(\hat{x}_1 - x_1) - rg_1(x_1)[\hat{x}_1 - x_1],\\ \dot{\hat{x}}_i &= \phi_{(i,i+1)}(x_1)\hat{x}_{i+1} - r^i g_i(x_1)[\hat{x}_1 - x_1]\ ,\ i = 2, \ldots, n-1,\\ \dot{\hat{x}}_n &= \mu_0(x_1)u - r^n g_n(x_1)[\hat{x}_1 - x_1],\end{aligned} \tag{12}$$

the observer errors can be defined as $e_i = \hat{x}_i - x_i, i = 1, \ldots, n$, and the scaled observer errors can be defined as $\epsilon_i = \frac{e_i}{r^{i-1}}, i = 1, \ldots, n$. The additional term involving $\frac{\dot{r}}{r}$ in $\dot{\hat{x}}_1$ in (12) is introduced to generate that the resulting D matrix in the scaled error dynamics (7) has a positive element in its $(1, 1)$ location and is thereby retained as a positive-definite matrix. The prescribed-time control design procedure in this article can be applied with either the reduced-order observer (9) or the full-order observer (12). While the structure of the full-order observer in (12) is somewhat simpler algebraically than the reduced-order observer in (9), parts of the control design and stability analysis are somewhat simpler with a reduced-order observer since we have one less state variable in the reduced-order observer. In this article, we utilize a reduced-order observer.

[4]The notation $\mathrm{diag}(T_1, \ldots, T_m)$ denotes an $m \times m$ diagonal matrix with diagonal elements $T_1, \ldots, T_m$. In addition, $\mathrm{lowerdiag}(T_1, \ldots, T_{m-1})$ and $\mathrm{upperdiag}(T_1, \ldots, T_{m-1})$ denote the $m \times m$ matrices with the lower diagonal entries (ie, $(i+1, i)$th entries, $i = 1, \ldots, m-1$) and upper diagonal entries (ie, $(i, i+1)$th entries, $i = 1, \ldots, m-1$), respectively, being $T_1, \ldots, T_{m-1}$ and zeros elsewhere. I_m denotes the $m \times m$ identity matrix.

3.2 | Dynamics of scaled observer estimate signals

Define $\eta_2, \ldots, \eta_n$ as

$$\eta_2 = \frac{\hat{x}_2 + rf_2(x_1) + \zeta(x_1, \hat{\theta})}{r}, \tag{13}$$

$$\eta_i = \frac{\hat{x}_i + r^{i-1}f_i(x_1)}{r^{i-1}}, i = 3, \ldots, n, \tag{14}$$

where the function ζ is defined to be of the form

$$\zeta(x_1, \hat{\theta}) = \hat{\theta}x_1\zeta_1(x_1) \tag{15}$$

with $\hat{\theta}$ being a dynamic adaptation parameter (whose dynamics will be designed below) and ζ_1 being a function that will be designed below. The dynamics designed for $\hat{\theta}$ will ensure that $\hat{\theta}(t) \geq 1$ for all $t \geq 0$.

3.3 | Design of control input *u* and dynamics of scaled states

The control input u is designed as

$$u = -\frac{r^n}{\mu_0(x_1)}K_c\eta \tag{16}$$

with[5] $K_c = [k_2, \ldots, k_n]$ where $k_2, \ldots, k_n$, are functions of x_1. Under the control law (16), the dynamics of $\eta = [\eta_2, \ldots, \eta_n]^T$ can be written as

$$\dot{\eta} = rA_c\eta - \frac{\dot{r}}{r}D\eta + \Phi - rG\epsilon_2 + H[\eta_2 - \epsilon_2] + \Xi \tag{17}$$

where A_c is the $(n-1)\times(n-1)$ matrix with (i,j)th element $A_{c_{(i,i+1)}}(x_1) = \phi_{(i+1,i+2)}(x_1)$ for $i = 1, \ldots, n-2$, and $A_{c_{(n-1,j)}}(x_1) = -k_{j+1}(x_1)$ for $j = 1, \ldots, n-1$, with zeros elsewhere. The matrix D is as defined in (8). In addition,

$$G = [g_2, \ldots, g_n]^T \quad ; \quad \Phi = \frac{\phi_1}{\phi_{(1,2)}}G, \tag{18}$$

$$H = [\hat{\theta}[\zeta_1'(x_1)x_1 + \zeta_1]\phi_{(1,2)}, 0, \ldots, 0]^T, \tag{19}$$

$$\Xi = [\frac{(\phi_1 - \zeta\phi_{(1,2)})\hat{\theta}[\zeta_1'(x_1)x_1 + \zeta_1] + \dot{\hat{\theta}}x_1\zeta_1(x_1)}{r}, 0, \ldots, 0]^T, \tag{20}$$

where $\zeta_1'(x_1)$ denotes the partial derivative of ζ_1 with respect to its argument evaluated at x_1.

Remark 3. The observer and controller structures in Sections 3.1 and 3.3 are based on the dual dynamic high-gain scaling based design methodology.[39] This underlying design methodology which was developed in the context of asymptotic stabilization in Reference 39 is based on viewing the observer error dynamics and control design problem using matrix structures (eg, Equations (7), (16), (17)) and designing observer and controller gains using pairs of coupled Lyapunov inequalities (Section 3.6). After designing the observer and controller gains, the remaining design freedoms (dynamics of r and $\hat{\theta}$, function ζ_1) are designed based on a Lyapunov analysis as discussed in Sections 3.7 to 3.9. The control design and analysis utilize the time scale transformation $\tau = a(t)$ defined in Section 3.4 that maps the finite time interval $[0, T)$ in terms of t to the infinite time interval $[0, \infty)$ in terms of τ so that achieving the desired convergence properties asymptotically as $\tau \to \infty$ effectively achieves the desired properties as t approaches the finite prescribed time T. Aspects of the proposed design procedure (eg, time scale transformation $\tau = a(t)$, decomposition of the prescribed time interval into a first phase in which the uncertain parameters in the system dynamics are dominated by some appropriate controller state

[5] For notational convenience, we drop the arguments of functions whenever no confusion will result.

variables in an initial subinterval of the prescribed time and a second phase in which the system state and input are regulated to 0 in the remaining part of the prescribed time interval) can be applied to other control design methodologies such as backstepping as well to address different classes of systems. The dual dynamic high-based scaling based control design methodology is used in this article for a few crucial reasons. First, while an application of the time scale transformation $\tau = a(t)$ to a backstepping design for system class (1) would need to deal with repeated derivatives of $\alpha(\tau)$ that would appear over multiple steps of backstepping leading to significant algebraic complexity, the one-step matrix-based controller design (16) based on coupled Lyapunov inequalities (Section 3.6) does not involve repeated differentiation of $\alpha(\tau)$. Second, the considered upper bounds on the uncertain functions ϕ_i in Assumption 2, which include crossproducts between uncertain parameters θ and unmeasured state variables $x_2, \ldots, x_n$ without requiring any a priori known upper bounds on the uncertain parameters, cannot be handled in a typical backstepping-based control design since the usual approach for introducing adaptations to handle uncertain parameters does not work when the uncertain parameters are multiplied with unmeasured state variables. In addition, the appearance of $x_2, \ldots, x_n$ in the upper bounds are not easily handled in an output-feedback backstepping based design since while backstepping can efficiently assign gains to the output, the gains to other states cannot be assigned arbitrarily since states farther from the output appear in increasingly complicated combinations in the recursive design procedure and generated Lyapunov function. Such terms can however be directly handled in the dual dynamic high-gain scaling based control design approach by writing these upper bounds in terms of matrix structures (Section 3.7) and designing the dynamics of the high-gain scaling parameter r appropriately to handle these terms (Section 3.9).

3.4 | Temporal scale transformation

As discussed in Remark 3, the control design and analysis are performed using a time scale transformation $\tau = a(t)$ which maps the finite time interval $[0, T)$ in terms of the original time variable t to the infinite time interval $[0, \infty)$ in terms of the new time variable τ. By designing the controller to achieve the desired convergence properties as $\tau \to \infty$, these properties are effectively achieved as $t \to T$ (ie, prescribed-time stabilization) since $\tau \to \infty$ is equivalent to $t \to T$ with the transformation $\tau = a(t)$. The choice of the function $a(\cdot)$ for this purpose is discussed below.

Let $a(\cdot)$ be a twice continuously differentiable monotonically increasing function over $[0, T)$ satisfying the following conditions (see Remark 4 below):

- $a(0) = 0$, $\lim_{t \to T} a(t) = \infty$
- $\frac{da}{dt}$ is bounded below by a positive constant over $[0, T)$, that is, $\frac{da}{dt} \geq a_0 > 0$ for $t \in [0, T)$ with a_0 being a constant
- Denoting the transformation $\tau = a(t)$ and writing $a'(t) \text{def=} \frac{da}{dt}$ as a function of τ as $\alpha(\tau) = \frac{da}{dt}$, $\alpha(\tau)$ grows at most polynomially as $\tau \to \infty$, that is, a polynomial $\overline{\alpha}(\tau)$ exists such that $\alpha(\tau) \leq \overline{\alpha}(\tau)$ for all $\tau \in [0, \infty)$. In addition, $\frac{d\alpha}{d\tau}$ grows at most polynomially as $\tau \to \infty$.

With τ defined as the transformation $\tau = a(t)$, we see that when t goes from 0 to T, τ goes from 0 to ∞. Now,

$$d\tau = a'(t)dt \tag{21}$$

where $a'(t)$ denotes $\frac{da}{dt}$. With the transformation $\tau = a(t)$, let $\alpha(\tau) = a'(t)$. The transformation above is a time scale transformation wherein the interval $[0, T)$ in terms of the time variable t corresponds to the interval $[0, \infty)$ in terms of the time variable τ. To denote a signal $x(t)$ as a function of transformed time variable τ, we use the notation $\breve{x}(\tau)$, that is, $x(t) = \breve{x}(\tau)$ since both $x(t)$ and $\breve{x}(\tau)$ refer to the value of the same signal at the same physical time point represented as t in the original time axis and τ in the transformed time axis. The conditions on the function $a : [0, T) \to [0, \infty)$ introduced above imply that this function is invertible. Denoting the inverse function by a^{-1}, we have, by definition,

$$x(t) = x(a^{-1}(\tau)) = \breve{x}(\tau) = \breve{x}(a(t)). \tag{22}$$

Remark 4. As noted in References 38,45, there are many (in fact, infinite number of) functions that satisfy the conditions defined for function a above. For example, we can pick a to be one of the following functions with a_0 being a positive constant:

$$a(t) = \frac{a_0 t}{1 - \frac{t}{T}}, \tag{23}$$

$$a(t) = \frac{a_0 t}{\sqrt{1 - (\frac{t}{T})^2}}, \tag{24}$$

$$a(t) = a_0 T \tan(1) \left(\frac{\sin(1)}{\sin\left(1 - \frac{t}{T}\right)} - 1 \right). \tag{25}$$

For $a(t)$ given in (23), we have:

$$a'(t) = \frac{a_0}{(1 - \frac{t}{T})^2} \;\; ; \; \alpha(\tau) = a_0 \left(\frac{\tau}{a_0 T} + 1 \right)^2. \tag{26}$$

For $a(t)$ given in (24), we have:

$$a'(t) = \frac{a_0}{(1 - (\frac{t}{T})^2)^{\frac{3}{2}}} \;\; ; \; \alpha(\tau) = a_0 \left(\frac{\tau}{a_0 T} + 1 \right)^{\frac{3}{2}}. \tag{27}$$

For $a(t)$ given in (25), we have:

$$a'(t) = \frac{a_0 \sin(1) \tan(1)}{\sin^2\left(1 - \frac{t}{T}\right)} \cos\left(1 - \frac{t}{T}\right) \;\; ; \; \alpha(\tau) = \frac{(\tau + a_0 T \sin(1)\tan(1))^2}{a_0 \sin(1)\tan(1) T^2} \sqrt{1 - \left(\frac{a_0 T \sin(1)\tan(1)}{\tau + a_0 T \sin(1)\tan(1)} \right)^2}. \tag{28}$$

◇

3.5 | Lyapunov functions

Define

$$V_o = r\epsilon^T P_o \epsilon \; ; \; V_c = \frac{1}{2} x_1^2 + r\eta^T P_c \eta \; ; \; V = cV_o + V_c, \tag{29}$$

where P_o and P_c are symmetric positive definite matrices to be defined later and c is a positive constant to be picked later. Using (7), (17), and (29), and noting that the temporal scale transformation defined above yields $dt = \frac{d\tau}{\alpha(\tau)}$, we have

$$\begin{aligned} \frac{dV}{d\tau} = \frac{1}{\alpha(\tau)} & \{ cr^2 \epsilon^T [P_o A_o + A_o^T P_o] \epsilon + 2rc\epsilon^T P_o \overline{\Phi} \\ & + x_1 [\phi_1 + (r\eta_2 - \zeta - r\epsilon_2)\phi_{(1,2)}] + r^2 \eta^T [P_c A_c + A_c^T P_c] \eta \\ & + 2r\eta^T P_c (\Phi - rG\epsilon_2 + H[\eta_2 - \epsilon_2] + \Xi) \} \\ & - \frac{dr}{d\tau} \{ c\epsilon^T [P_o \tilde{D} + \tilde{D} P_o] \epsilon + \eta^T [P_c \tilde{D} + \tilde{D} P_c] \eta \}, \end{aligned} \tag{30}$$

where $\tilde{D} = D - \frac{1}{2} I$ with I denoting an identity matrix of dimension $(n-1) \times (n-1)$.

3.6 | Coupled Lyapunov inequalities

Assumption 3 is the *cascading dominance* condition introduced in Reference 39 wherein the condition in (3) is the "controller-context" cascading dominance condition and the condition in (4) is the "observer-context" cascading dominance condition. These cascading dominance conditions were shown in References 39,47,48 to be closely related to solvability of pairs of coupled Lyapunov inequalities that appear in the high-gain based control design. Specifically, the following lemmas follow from the construction for solution of coupled Lyapunov inequalities in References 39,47,48.

Lemma 1. *Under Assumption 1 and the condition (3) in Assumption 3, a symmetric positive definite matrix P_c and a function $K_c(x_1) = [k_2(x_1), \dots, k_n(x_1)]$ (whose elements appear in the definition of the matrix A_c) can be constructed such that the following coupled Lyapunov inequalities are satisfied (for all $x_1 \in \mathcal{R}$) with some positive constants ν_c, $\underline{\nu}_c$, and $\overline{\nu}_c$:*

$$\begin{aligned} P_c A_c + A_c^T P_c &\leq -\nu_c \phi_{(2,3)} I \\ \underline{\nu}_c I \leq P_c \tilde{D} + \tilde{D} P_c &\leq \overline{\nu}_c I. \end{aligned} \tag{31}$$

Proof. This lemma follows directly from theorem A2 in Reference 39. The matrix A_c can be viewed as a special case of the matrix $\tilde{A}$ in theorem A2 in Reference 39 with nonzero entries only on the upper diagonal and the last row. In addition, the matrix $\tilde{D}$ is a special case of the diagonal matrix $\tilde{D}$ in theorem A2 in Reference 39 with positive constant entries on its diagonal instead of the more general case of state-dependent entries in theorem A2 in Reference 39. ■

Lemma 2. *Under Assumption 1 and condition (4) in A3, a symmetric positive-definite matrix P_o and a function $G(x_1) = [g_2(x_1), \dots, g_n(x_1)]$ (whose elements appear in the definition of the matrix A_o) can be constructed such that the following coupled Lyapunov inequalities are satisfied (for all $x_1 \in \mathcal{R}$) with some positive constants ν_o, $\tilde{\nu}_o$, $\underline{\nu}_o$, and $\overline{\nu}_o$:*

$$\begin{aligned} P_o A_o + A_o^T P_o &\leq -\nu_o I - \tilde{\nu}_o \phi_{(2,3)} C^T C \\ \underline{\nu}_o I \leq P_o \tilde{D} + \tilde{D} P_o &\leq \overline{\nu}_o I, \end{aligned} \tag{32}$$

where $C = [1, 0, \dots, 0]$. Furthermore, $g_2, \dots, g_n$ can be chosen to be linear constant-coefficient combinations of $\phi_{(2,3)}, \dots, \phi_{(n-1,n)}$, and a positive constant $\overline{G}$ can be found such that the following inequality is satisfied:

$$\left(\sum_{i=2}^{n} g_i^2 \right)^{\frac{1}{2}} \leq \overline{G} \phi_{(2,3)}. \tag{33}$$

Proof. The existence of a symmetric positive-definite matrix P_o and functions $g_2, \dots, g_n$ follows directly from theorem A1 in Reference 39. Similar to Lemma 1, the matrix A_o can be viewed as a special case of the matrix A in theorem A1 in Reference 39 with nonzero entries only on the upper diagonal and the first column and the matrix $\tilde{D}$ can be viewed as a special case of the diagonal matrix D in theorem A1 in Reference 39 with positive constant entries on its diagonal instead of state-dependent entries. In addition, from theorem A1 in Reference 39, it is seen that $g_2, \dots, g_n$ can be chosen to be linear constant-coefficient combinations of $\phi_{(2,3)}, \dots, \phi_{(n-1,n)}$. From Assumption 3 (cascading dominance of upper diagonal terms $\phi_{(i,i+1)}$), we have the inequalities $\phi_{(i,i+1)}(x_1) \leq \underline{\rho}_i \, \phi_{(i-1,i)}(x_1), i = 3, \dots, n-1$, which imply $\phi_{(i,i+1)}(x_1) \leq (\prod_{j=3}^{i} \underline{\rho}_j) \phi_{(2,3)}(x_1), i = 3, \dots, n-1$. Hence, all the functions $\phi_{(i,i+1)}$ can be upper bounded, up to a multiplicative constant, by $\phi_{(2,3)}$ therefore implying that a positive constant $\overline{G}$ exists such that (33) is satisfied. ■

The symmetric positive-definite matrices P_o and P_c and the functions $g_2, \dots, g_n$, and $k_2, \dots, k_n$, are picked in accordance with Lemmas 1 and 2. Using (31) and (32), (30) reduces to

$$\begin{aligned} \frac{dV}{d\tau} = \frac{1}{\alpha(\tau)} \{ & -cr^2 \nu_o |\epsilon|^2 - cr^2 \tilde{\nu}_o \phi_{(2,3)} \epsilon_2^2 - r^2 \nu_c \phi_{(2,3)} |\eta|^2 \\ & + 2rc\epsilon^T P_o \overline{\Phi} + x_1 [\phi_1 + (r\eta_2 - \zeta - r\epsilon_2)\phi_{(1,2)}] \\ & + 2r\eta^T P_c (\Phi - rG\epsilon_2 + H[\eta_2 - \epsilon_2] + \Xi) \} \\ & - c\frac{dr}{d\tau} \underline{\nu}_o |\epsilon|^2 - \frac{dr}{d\tau} \underline{\nu}_c |\eta|^2. \end{aligned} \tag{34}$$

3.7 | Inequality bounds on terms appearing in $\frac{dV}{d\tau}$

Using Assumption 2, (15), and (33), we obtain

$$|\overline{\Phi}| \leq \theta \frac{\Gamma(x_1)|x_1|}{r}[|\tilde{\phi}_1| + |\hat{\theta}\zeta_1(x_1)||\tilde{\phi}_2|] + \theta\Gamma(x_1)||\tilde{A}(x_1)||(|\eta| + |\epsilon|) + \theta\Gamma(x_1)|x_1|\frac{\phi_{(1,1)}(x_1)}{\phi_{(1,2)}(x_1)}\overline{G}\phi_{(2,3)}(x_1), \tag{35}$$

where $\tilde{\phi}_1 = [\phi_{(2,1)}, \phi_{(3,1)}, \ldots, \phi_{(n,1)}]^T$, $\tilde{\phi}_2 = [\phi_{(2,2)}, \phi_{(3,2)}, \ldots, \phi_{(n,2)}]^T$, $||.||$ denotes the Frobenius norm of a matrix, and $\tilde{A}$ denotes the $(n-1)\times(n-1)$ matrix with (i,j)th element $\phi_{(i+1,j+1)}$ at locations on and below the diagonal and zeros everywhere else. Note that $|\tilde{\phi}_1| = \sqrt{\sum_{i=2}^{n}\phi_{(i,1)}^2(x_1)}$ and $|\tilde{\phi}_2| = \sqrt{\sum_{i=2}^{n}\phi_{(i,2)}^2(x_1)}$.

Therefore, the term $2rc\epsilon^T P_o\overline{\Phi}$ can be upper bounded as[6]

$$2rc\epsilon^T P_o\overline{\Phi} \leq \zeta_0\phi_{(1,2)}x_1^2 + 3rc\lambda_{\max}(P_o)\theta\Gamma||\tilde{A}||(|\eta|^2 + |\epsilon|^2) + \frac{c^2\lambda_{\max}^2(P_o)|\epsilon|^2}{\zeta_0\phi_{(1,2)}}\theta^2\Gamma^2[|\tilde{\phi}_1| + |\hat{\theta}\zeta_1||\tilde{\phi}_2|]^2 + 4c\lambda_{\max}^2(P_o)\theta^2\Gamma^2x_1^2\frac{\phi_{(1,1)}^2}{\phi_{(1,2)}^2}\overline{G}^2\phi_{(2,3)}^2 + \frac{c}{4}r^2v_o|\epsilon|^2, \tag{36}$$

where $\zeta_0 > 0$ is any constant. Using Assumptions 1 to 3 and property $r \geq 1$, the other uncertain terms appearing in (30) can also be upper bounded as

$$x_1\phi_1 \leq x_1^2\theta\Gamma(x_1)\phi_{(1,1)}(x_1), \tag{37}$$

$$x_1r(\eta_2 - \epsilon_2)\phi_{(1,2)} \leq \frac{v_c}{4}r^2\phi_{(2,3)}|\eta|^2 + \frac{1}{v_c}x_1^2\frac{\phi_{(1,2)}^2}{\phi_{(2,3)}} + cr^2\frac{\tilde{v}_o}{4}\phi_{(2,3)}\epsilon_2^2 + \frac{1}{c\tilde{v}_o}x_1^2\frac{\phi_{(1,2)}^2}{\phi_{(2,3)}}, \tag{38}$$

$$2r\eta^T P_c\Phi \leq \frac{4}{v_c}\lambda_{\max}^2(P_c)\overline{G}^2\frac{\phi_{(2,3)}}{\phi_{(1,2)}^2}\theta^2\Gamma^2\phi_{(1,1)}^2x_1^2 + \frac{v_c}{4}r^2\phi_{(2,3)}|\eta|^2, \tag{39}$$

$$-2r^2\eta^T P_cG\epsilon_2 \leq \frac{8}{v_c}\phi_{(2,3)}r^2\lambda_{\max}^2(P_c)\overline{G}^2\epsilon_2^2 + r^2\frac{v_c}{8}\phi_{(2,3)}|\eta|^2, \tag{40}$$

$$2r\eta^T P_cH(\eta_2 - \epsilon_2) \leq 3r\lambda_{\max}(P_c)\hat{\theta}\phi_{(1,2)}|\zeta_1'x_1 + \zeta_1|[|\eta|^2 + |\epsilon|^2], \tag{41}$$

$$2r\eta^T P_c\Xi \leq \frac{2}{\zeta_0\phi_{(1,2)}}\lambda_{\max}^2(P_c)|\eta|^2\left[\dot{\hat{\theta}}^2\zeta_1^2 + (\theta\Gamma\phi_{(1,1)} + |\zeta_1|\hat{\theta}\phi_{(1,2)})^2(\zeta_1'x_1 + \zeta_1)^2\hat{\theta}^2\right] + \zeta_0\phi_{(1,2)}x_1^2. \tag{42}$$

Picking $c \geq \frac{32\lambda_{\max}^2(P_c)\overline{G}^2}{3\tilde{v}_o v_c}$, the inequality (40) reduces to

$$-2r^2\eta^T P_cG\epsilon_2 \leq r^2\frac{v_c}{8}\phi_{(2,3)}|\eta|^2 + \frac{3}{4}c\tilde{v}_o\phi_{(2,3)}r^2\epsilon_2^2. \tag{43}$$

3.8 | Lyapunov analysis

Using (31), (32), and the inequalities in (36) to (43), (34) yields

$$\frac{dV}{d\tau} \leq \frac{1}{\alpha(\tau)}\{-x_1^2\hat{\theta}\zeta_1\phi_{(1,2)} - \frac{3}{4}v_ocr^2|\epsilon|^2 - \frac{3}{8}v_c\phi_{(2,3)}r^2|\eta|^2 + q_1(x_1)\phi_{(1,2)}x_1^2 + \theta^*q_2(x_1)\phi_{(1,2)}x_1^2 + r[w_1(x_1,\hat{\theta},\dot{\hat{\theta}}) + \theta^*w_2(x_1,\hat{\theta})]\phi_{(1,2)}[|\eta|^2 + |\epsilon|^2]\} - c\underset{-o}{v}\frac{dr}{d\tau}|\epsilon|^2 - \underset{-c}{v}\frac{dr}{d\tau}|\eta|^2, \tag{44}$$

[6]Given a symmetric positive-definite matrix P, $\lambda_{\max}(P)$ and $\lambda_{\min}(P)$ denote its maximum and minimum eigenvalues, respectively.

where $\theta^* = 1 + \theta + \theta^2$ and the functions $q_1(x_1)$, $q_2(x_1)$, $w_1(x_1, \hat{\theta}, \dot{\hat{\theta}})$, and $w_2(x_1, \hat{\theta})$ are as given in (45) to (48) below:

$$q_1(x_1) = 2\zeta_0 + \frac{1}{\nu_c}\frac{\phi_{(1,2)}(x_1)}{\phi_{(2,3)}(x_1)} + \frac{1}{c\tilde{\nu}_o}\frac{\phi_{(1,2)}(x_1)}{\phi_{(2,3)}(x_1)}, \tag{45}$$

$$q_2(x_1) = \Gamma(x_1)\frac{\phi_{(1,1)}(x_1)}{\phi_{(1,2)}(x_1)} + 4c\lambda_{\max}^2(P_o)\Gamma^2(x_1)\frac{\phi_{(1,1)}^2(x_1)}{\phi_{(1,2)}^3(x_1)}\overline{G}^2\phi_{(2,3)}^2(x_1) + \frac{4}{\nu_c}\lambda_{\max}^2(P_c)\overline{G}^2\frac{\phi_{2,3}(x_1)}{\phi_{(1,2)}^3(x_1)}\Gamma^2(x_1)\phi_{(1,1)}^2(x_1), \tag{46}$$

$$w_1(x_1, \hat{\theta}, \dot{\hat{\theta}}) = \frac{2}{\zeta_0\phi_{(1,2)}^2(x_1)}\lambda_{\max}^2(P_c)\left[\dot{\hat{\theta}}^2\zeta_1^2(x_1) + 2(|\zeta_1(x_1)|\hat{\theta}\phi_{(1,2)}(x_1))^2(\zeta_1'(x_1)x_1 + \zeta_1(x_1))^2\hat{\theta}^2\right]$$
$$+ 3\lambda_{\max}(P_c)\hat{\theta}|\zeta_1'(x_1)x_1 + \zeta_1(x_1)|, \tag{47}$$

$$w_2(x_1, \hat{\theta}) = \frac{c^2\lambda_{\max}^2(P_o)}{\zeta_0\phi_{(1,2)}^2(x_1)}\Gamma^2(x_1)[|\tilde{\phi}_1(x_1)| + |\hat{\theta}\zeta_1(x_1)||\tilde{\phi}_2(x_1)|]^2 + 3c\frac{\lambda_{\max}(P_o)}{\phi_{(1,2)}(x_1)}\Gamma(x_1)||\tilde{A}(x_1)||$$
$$+ \frac{4}{\zeta_0\phi_{(1,2)}^2(x_1)}\lambda_{\max}^2(P_c)\left[(\Gamma(x_1)\phi_{(1,1)}(x_1))^2(\zeta_1'(x_1)x_1 + \zeta_1(x_1))^2\hat{\theta}^2\right]. \tag{48}$$

Note that the functions $q_1(x_1)$, $q_2(x_1)$, $w_1(x_1, \hat{\theta}, \dot{\hat{\theta}})$, and $w_2(x_1, \hat{\theta})$ involve only known functions and quantities. In the equations above, note that $\dot{\hat{\theta}}$ denotes $\frac{d\hat{\theta}}{dt}$. We have $\frac{d\hat{\theta}}{d\tau} = \frac{1}{\alpha(\tau)}\frac{d\hat{\theta}}{dt}$.

Remark 5. In (44), the terms in the first line are nonpositive functions of x_1, ϵ, and η, respectively, and can therefore be seen to be stabilizing terms in the context of the Lyapunov inequality (44). The terms in the third line of (44) can be made nonpositive by suitably choosing $\frac{dr}{d\tau}$. The terms in the second line are nonnegative (ie, destabilizing) terms, which would need to be somehow dominated by the terms in the first and third lines. The design freedoms that are available to us for this purpose are the function ζ_1 and the dynamics of r and $\hat{\theta}$, that is, $\frac{dr}{d\tau}$ and $\frac{d\theta}{d\tau}$. The goal in this design as will be seen below is to pick function ζ_1 and the dynamics of r and $\hat{\theta}$ so that in some time interval $\tau \in [\tau_0, \infty)$ with some $\tau_0 < \infty$, the inequality $\frac{dV}{d\tau} \leq -\kappa V$ is satisfied with some $\kappa > 0$. As will be seen in Section 4, achieving such an inequality will imply that $x_1, x_2, \ldots, x_n, \hat{x}_2, \ldots, \hat{x}_n$ go to 0 exponentially as $\tau \to \infty$, that is, as $t \to T$. Also will be seen in Section 4, ensuring that r and $\hat{\theta}$ grow at most polynomially in τ will furthermore imply that u goes to 0 exponentially as $\tau \to \infty$, that is, as $t \to T$. In the design below, the function ζ_1 will be picked (as shown in (49)) to address the terms involving q_1 and q_2 (but with an adaptation parameter $\hat{\theta}$ in place of the uncertain parameter θ^*). The form of $\frac{dr}{d\tau}$ will then be designed to address the terms involving w_1 and w_2 (but with a fractional power r^b introduced to take the place of θ^*). The dynamics of $\hat{\theta}$ and r will then be designed to make $\hat{\theta}$ and r^b able to dominate the uncertain parameter θ^* quickly enough (ie, within a subinterval of the prescribed time interval $[0, T)$ which in terms of the transformed time variable τ maps to $[0, \infty)$ and to thereby make the system state and input exponentially converge to zero within the remaining subinterval of the prescribed time interval. In this context, it is to be noted that the typical approach in adaptive control of using a Lyapunov function such as $\overline{V} = V + \frac{1}{2}(\hat{\theta} - \theta^*)^2$ to design the dynamics of $\hat{\theta}$ to handle the $\theta^* w_2(x_1, \hat{\theta})\phi_{(1,2)}[|\eta^2| + |\epsilon|^2]$ term will not work since ϵ is not measured. Specifically, such an approach would lead to the adaptation dynamics $\frac{d\hat{\theta}}{d\tau} = \frac{1}{\alpha(\tau)}[q_2(x_1)\phi_{(1,2)}x_1^2 + rw_2(x_1, \hat{\theta})\phi_{(1,2)}(|\eta|^2 + |\epsilon|^2)]$, which cannot be implemented since ϵ is not available. Instead, the approach here is to use the fact that $\hat{\theta}$ and r grow with τ (due to the designed dynamics of $\hat{\theta}$ and r) to dominate θ^* after some finite time. Hence, as will be seen in (57), the Lyapunov inequality (44) will be rewritten after the design of the function ζ_1 and the dynamics of $\hat{\theta}$ and r in a form involving terms with coefficients $(\theta^* - \hat{\theta})$ and $(\theta^* - r)$, both of which become nonpositive after some finite time since $\hat{\theta}$ and r grow unbounded with τ.

3.9 | Designs of function ζ_1 and dynamics of r and $\hat{\theta}$

The function ζ_1 is designed such that[7]

$$\frac{1}{4}\zeta_1(x_1) = \max\{\underline{\zeta}, q_1(x_1) + q_2(x_1)\} \tag{49}$$

[7]The notations $\max(a_1, \ldots, a_n)$ and $\min(a_1, \ldots, a_n)$ indicate the largest and smallest values, respectively, among the numbers $a_1, \ldots, a_n$.

with ζ being any positive constant. With the choice of the function ζ_1 in (49), we obtain the following inequality by noting that $\hat{\theta} \geq 1$ for all time:

$$\begin{aligned}\hat{\theta}\zeta_1(x_1) - q_1(x_1) - \theta^* q_2(x_1) &\geq \frac{3}{4}\hat{\theta}\zeta_1(x_1) + \hat{\theta}[q_1(x_1) + q_2(x_1)] - q_1(x_1) - \theta^* q_2(x_1) \\ &\geq \frac{3}{4}\hat{\theta}\zeta_1(x_1) + (\hat{\theta} - \theta^*)q_2(x_1). \end{aligned} \tag{50}$$

The dynamics of r are designed to be of the form

$$\begin{aligned}\frac{dr}{d\tau} &= \frac{1}{\alpha(\tau)} \max\{-c_0 r(r - \max\{1, \alpha(\tau)\} - c_1) + \Omega(r, x_1, \hat{\theta}, \dot{\hat{\theta}}) + \tilde{\alpha}(\tau)\alpha(\tau)\ ,\ 0\} \\ &\quad \text{with } \ r(0) > \max\{1, \alpha(0)\}, \end{aligned} \tag{51}$$

where $\tilde{\alpha}(\tau)$ denotes $\frac{d\alpha}{d\tau}$, c_1 is any nonnegative constant, and c_0 and Ω are a positive constant and a function, respectively, picked as

$$c_0 = \min\left\{\frac{v_o}{2\underline{v}_o}, \frac{v_c\sigma}{4\underline{v}_c}\right\} \tag{52}$$

$$\Omega(r, x_1, \hat{\theta}, \dot{\hat{\theta}}) = r[w_1(x_1, \hat{\theta}, \dot{\hat{\theta}}) + r^b w_2(x_1, \hat{\theta})]\phi_{(1,2)}(x_1) \max\left\{\frac{1}{c\underline{v}_o}, \frac{1}{\underline{v}_c}\right\}, \tag{53}$$

where b is any constant in the interval $(0, 1)$. It is seen that the positive constant c_0 is picked in (52) to be "small enough" so that the stabilizing $-r^2$ term in $\frac{dr}{d\tau}$ fits within the "margin" provided by the $-r^2$ terms in $\frac{dV}{d\tau}$ in (44). In addition, as will be seen in Lemmas 4 and 5 in Section 4, the $-r^2$ term in the dynamics of r is crucial to ensure that r does not grow "too fast" in the time τ and in particular, that r grows at most polynomially in τ. Furthermore, it will be seen in Lemma 8 in Section 4 that the fact that r grows at most polynomially is crucial in showing that $u \to 0$ as $\tau \to \infty$ by using the fact that a product of polynomial and exponentially decaying terms converges to zero. From the design of the dynamics of r, we also see that $\frac{dr}{d\tau} \geq 0$ for all $\tau \geq 0$. In addition, from (51), it is seen that the inequality $\frac{dr}{d\tau} \geq \tilde{\alpha}(\tau)$ definitely holds at any time instant at which $r \leq \max\{1, \alpha(\tau)\} + c_1$. It is seen below in Lemma 3 that the form of the dynamics of r given above implies that $r \geq \alpha(\tau)$ for all τ in the maximal interval of existence of solutions.

The dynamic adaptation parameter $\hat{\theta}$ is defined to be comprised of two components, that is,

$$\hat{\theta} = \hat{\theta}_1 + \hat{\theta}_2 \tag{54}$$

and the dynamics of $\hat{\theta}_1$ and $\hat{\theta}_2$ are designed as

$$\frac{d\hat{\theta}_1}{d\tau} = \tilde{\alpha}(\tau) \text{ with } \ \hat{\theta}_1(0) \geq \max\{1, \alpha(0)\}, \tag{55}$$

$$\frac{d\hat{\theta}_2}{d\tau} = \frac{c_\theta}{\alpha(\tau)} q_2(x_1)\phi_{(1,2)}(x_1)x_1^2 \text{ with } \ \hat{\theta}_2(0) \geq 0, \tag{56}$$

where c_θ is any positive constant. From (55) and (56), we see that $\hat{\theta}_1 \geq \alpha(\tau)$ and $\hat{\theta}_2 \geq 0$ for all τ for all τ in the maximal interval of existence of solutions. Hence, we also have $\hat{\theta} \geq \alpha(\tau)$ for all τ in the maximal interval of existence of solutions. As noted above, the dynamics of r in (51) also ensures that $r \geq \alpha(\tau)$ for all τ in the maximal interval of existence of solutions. The fact that r and θ are both larger than or equal to $\alpha(\tau)$ for all times τ is relevant in the context of (44) since this implies that the r or $\hat{\theta}$ coefficients appearing in each of the terms in the first two lines of (44) dominate over the $\alpha(\tau)$ term appearing in the denominator in (44).

From the design of the dynamics of r in (51) with c_0 and Ω as in (52)and (53), we see that (44) reduces to

$$\frac{dV}{d\tau} \leq \frac{1}{\alpha(\tau)}\left\{-\frac{3}{4}x_1^2\hat{\theta}\zeta_1\phi_{(1,2)} - \frac{1}{4}\nu_o c r^2|\epsilon|^2 - \frac{1}{8}\nu_c\phi_{(2,3)}r^2|\eta|^2\right\} + (\theta^* - \hat{\theta})\chi_1(x_1,\tau) + (\theta^* - r^b)\chi_2(x_1,\hat{\theta},\tau)r[|\eta|^2 + |\epsilon|^2], \tag{57}$$

$$\chi_1(x_1,\tau) = \frac{1}{\alpha(\tau)}q_2(x_1)\phi_{(1,2)}(x_1)x_1^2, \tag{58}$$

$$\chi_2(x_1,\hat{\theta},\tau) = \frac{1}{\alpha(\tau)}w_2(x_1,\hat{\theta})\phi_{(1,2)}(x_1). \tag{59}$$

Hence, comparing with the definition of V in (29) and noting as discussed above that the dynamics of $\hat{\theta}$ implies that $\hat{\theta} \geq \alpha(\tau)$ for all τ, (57) yields

$$\frac{dV}{d\tau} \leq -\kappa V + (\theta^* - \hat{\theta})\chi_1(x_1,\tau) + (\theta^* - r^b)\chi_2(x_1,\hat{\theta},\tau)r[|\eta|^2 + |\epsilon|^2], \tag{60}$$

$$\kappa = \min\left\{\frac{3\zeta\underline{\sigma}}{2}, \frac{\nu_o}{4\lambda_{\max}(P_o)}, \frac{\nu_c\sigma}{8\lambda_{\max}(P_c)}\right\}. \tag{61}$$

4 | MAIN RESULT AND PROOF

Theorem 1. *Given a prescribed time $T > 0$ that can be picked arbitrarily by the control designer, a dynamic output-feedback controller of the form $u = f(\psi, y)$; $\dot{\psi} = g(\psi, y)$ can be designed for system (1) under Assumptions 1 to 3 such that starting from any initial condition for x, the property* $\lim_{t\to T}|x(t)| = \lim_{t\to T}|u(t)| = 0$ *is satisfied.*

In this section, we prove Theorem 1 based on the control design developed in Section 3 by first showing that the solutions to the closed-loop dynamical system exist for all time $\tau \in [0, \infty)$ and then showing that $\hat{\theta}$ and r grow large enough quickly enough in order to dominate the uncertain parameter θ^* in (60) within a subinterval of the prescribed time interval, (which is $[0, T)$ in terms of the time variable t or equivalently $[0, \infty)$ in terms of the time variable τ), and then finally showing that V (and therefore, x, u, and so on) converge to zero exponentially within the remaining subinterval of the prescribed time interval.

Lemma 3. *The signal r satisfies*[8] *the inequality $\check{r}(\tau) \geq \alpha(\tau)$ for all τ in the maximal interval of existence of solutions.*

Proof. From (51), we note that $\frac{dr}{d\tau} \geq \tilde{\alpha}(\tau)$ at any time instant at which $r \geq \max\{1, \alpha(\tau)\} + c_1$ is not satisfied. If the claim in Lemma 3 is not satisfied, there should exist some time instants τ at which $\check{r}(\tau) < \alpha(\tau)$. Let $\tau_{\min}$ be the infimum of all such time instants. Then, we note that since $r(0) > \alpha(0)$ from (51), we should have $\tau_{\min} > 0$ and we should also have $\check{r}(\tau_{\min}) = \alpha(\tau_{\min})$ and furthermore, for all τ in an open interval $(\tau_{\min}, \tau_{\min} + \delta)$ with some sufficiently small $\delta > 0$, the inequality $\check{r}(\tau) < \alpha(\tau)$ should hold. However, $\check{r}(\tau_{\min}) = \alpha(\tau_{\min})$ implies $\frac{dr}{d\tau} \geq \tilde{\alpha}(\tau) = \frac{d\alpha}{d\tau}$. Hence, we should have $\check{r}(\tau) \geq \alpha(\tau)$ for all τ over an open interval $(\tau_{\min}, \tau_{\min} + \tilde{\delta})$ with some sufficiently small $\tilde{\delta} > 0$. We therefore obtain a contradiction thereby implying that the claim of Lemma 3 is satisfied. ◇ ∎

Lemma 4. *A function $R(x_1, \hat{\theta}, \dot{\hat{\theta}}, \tau)$ exists such that the dynamics of r in (51) imply that $\frac{dr}{d\tau} = 0$ whenever $r \geq R(x_1, \hat{\theta}, \dot{\hat{\theta}}, \tau)$.*

[8]Note that, as defined in (22), the notation $\check{r}(\tau)$ indicates the value of the signal r at the time instant τ as measured in the transformed time axis, that is, $r(t) = \check{r}(\tau)$.

Proof. Defining $R(x_1, \hat{\theta}, \dot{\hat{\theta}}, \tau)$ to be of the form $\max\{3R_1(x_1, \hat{\theta}, \dot{\hat{\theta}}, \tau), (3R_2(x_1, \hat{\theta}))^{\frac{1}{1-b}}, \sqrt{3R_3(\tau)}\}$, the inequality $r \geq R$ implies $r^2 \geq R_1 r + R_2 r^{1+b} + R_3$. Now, defining

$$R_1(x_1, \hat{\theta}, \dot{\hat{\theta}}, \tau) = \max\{1, \alpha(\tau)\} + c_1 + w_1(x_1\hat{\theta}, \dot{\hat{\theta}})\tilde{c}_0, \tag{62}$$

$$R_2(x_1, \hat{\theta}) = w_2(x_1, \hat{\theta})\tilde{c}_0, \tag{63}$$

$$R_3(\tau) = \frac{\tilde{\alpha}(\tau)\alpha(\tau)}{c_0}, \tag{64}$$

with $\tilde{c}_0 = \frac{1}{c_0} \max\{\frac{1}{c_{\underline{v}_o}}, \frac{1}{\underline{v}_c}\}$, it is seen from the dynamics of r in (51) and the definition of Ω in (53) that this implies that $\frac{dr}{d\tau} = 0$ whenever $r \geq R(x_1, \hat{\theta}, \dot{\hat{\theta}}, \tau)$. ◇ ∎

Lemma 5. *If x_1 is uniformly bounded over the maximal interval of existence of solutions, then the signals $\hat{\theta}(a^{-1}(\tau))$, $\dot{\hat{\theta}}(a^{-1}(\tau))$, and $r(a^{-1}(\tau))$ grow at most polynomially in τ.*

Proof. By the dynamics of $\hat{\theta}_1$ in (55) and the conditions on function $\alpha(\tau)$, we see that $\hat{\theta}_1(a^{-1}(\tau))$ and $\dot{\hat{\theta}}_1(a^{-1}(\tau))$ are polynomially upper bounded in τ. If x_1 is uniformly bounded over the maximal interval of existence of solutions, we see that from the dynamics of $\hat{\theta}_2$ in (56), it follows that $\hat{\theta}_2(a^{-1}(\tau))$ and $\dot{\hat{\theta}}_2(a^{-1}(\tau))$ are also polynomially upper bounded in τ. Noting that $\hat{\theta}$ and $\dot{\hat{\theta}}$ appear polynomially in the definitions of w_1 and w_2 and that $\alpha(\tau)$ and $\tilde{\alpha}(\tau)$ are polynomially upper bounded in τ due to the conditions imposed on $\alpha(\tau)$ in Section 3.4, it follows that the $R(x_1, \hat{\theta}, \dot{\hat{\theta}}, \tau)$ constructed in Lemma 4 grows at most polynomially as a function of time τ. Hence, since, from Lemma 4, $\frac{dr}{d\tau} = 0$ whenever $r \geq R(x_1, \hat{\theta}, \dot{\hat{\theta}}, \tau)$, it is seen that $r(a^{-1}(\tau))$ grows at most polynomially as a function of time τ. ◇ ∎

Lemma 6. *Solutions to the closed-loop dynamical system formed by (1) and the designed dynamic controller exist over time interval $\tau \in [0, \infty)$. V is uniformly bounded over the time interval $\tau \in [0, \infty)$. The signals $\hat{\theta}(a^{-1}(\tau))$, $\dot{\hat{\theta}}(a^{-1}(\tau))$, and $r(a^{-1}(\tau))$ grow at most polynomially in τ as $\tau \to \infty$.*

Proof. Define $\overline{V} = V + \frac{1}{c_\theta}(\hat{\theta}_2 - \theta^*)^2$. Noting from (56) that we have $\frac{d\hat{\theta}_2}{d\tau} = c_\theta \chi_1(x_1, \tau)$ where $\chi_1(x_1, \tau)$ is as defined in (58), and noting that $\hat{\theta}_1 \geq 0$ for all τ and that $\chi_1(x_1, \tau) \geq 0$ for all x_1 and τ, it is seen from (60) that

$$\frac{d\overline{V}}{d\tau} \leq -\kappa V + (\theta^* - r^b)\chi_2(x_1, \hat{\theta}, \tau) r[|\eta|^2 + |\epsilon|^2]. \tag{65}$$

Denote the maximal interval (in terms of the τ time variable) of existence of solutions by $[0, \tau_f)$. We will show below by contradiction that $\tau_f = \infty$. Assuming τ_f is finite, consider the two Cases (note that r is monotonically nondecreasing): (C1) $\lim_{\tau \to \tau_f} r^b > \theta^*$; (C2) $\lim_{\tau \to \tau_f} r^b \leq \theta^*$.

Under Case (C1), a time $\underline{\tau}_f < \tau_f$ should exist such that $r^b \geq \theta^*$ for all $\tau \in [\underline{\tau}_f, \tau_f)$. Then, for all $\tau \in [\underline{\tau}_f, \tau_f)$, we should have $\frac{d\overline{V}}{d\tau} \leq -\kappa V$ implying that $\overline{V}$ and therefore V (and therefore also x_1) remain bounded on the maximal interval of existence of solutions. Hence, by Lemma 5, $\hat{\theta}(a^{-1}(\tau))$, $\dot{\hat{\theta}}(a^{-1}(\tau))$, and $r(a^{-1}(\tau))$ grow at most polynomially in τ. Therefore, under Case (C1), we see that all closed-loop signals remain bounded over any finite time interval $[0, \tau_f)$. Hence, solutions to the closed-loop dynamical system exist over the time interval $\tau \in [0, \infty)$.

Under Case (C2), we see by using the dynamics of r in (51), the definition of Ω in (53), the definition of χ_2 in (59), and the observations that $r \geq 1$ and $\alpha(\tau) \geq a_0$ for all time, that

$$\frac{dr}{d\tau} \geq -\frac{c_0}{a_0}(\theta^*)^{\frac{2}{b}} + \underline{c}\chi_2(x_1, \hat{\theta}, \tau), \tag{66}$$

where $\underline{c} = \max\{\frac{1}{c_{\underline{v}_o}}, \frac{1}{\underline{v}_c}\}$. Hence, under the hypothesis of Case (C2), it follows that $\int_0^{\tau_f} \chi_2(x_1, \hat{\theta}, \tau) d\tau \leq M$ with some finite M if τ_f is finite. From (65), the definition of V in (29), and the definition of $\overline{V}$ above, it is seen, by noting that $r \geq 0$, that

$$\frac{d\overline{V}}{d\tau} \leq \theta^* \chi_2(x_1, \hat{\theta}, \tau)\overline{\kappa}\overline{V}, \tag{67}$$

where $\overline{\kappa} = \max\{\frac{1}{\lambda_{\min}(P_c)}, \frac{1}{c\lambda_{\min}(P_o)}\}$. Hence, boundedness of $\overline{V}$ over a time interval $[0, \tau_f)$ with finite τ_f follows from boundedness of $\int_0^{\tau_f} \chi_2(x_1, \hat{\theta}, \tau)d\tau \leq M$. Similar to Case (C1) above, it is then seen that boundedness of $\overline{V}$ implies that V and x_1 are bounded over the maximal interval of existence of solutions and that the signals $\hat{\theta}(a^{-1}(\tau))$, $\dot{\hat{\theta}}(a^{-1}(\tau))$, and $r(a^{-1}(\tau))$ grow at most polynomially in τ, all closed-loop signals remain bounded over a finite time interval $[0, t_f)$, and that solutions to the closed-loop dynamical system exist over the time interval $\tau \in [0, \infty)$. ◇ ∎

Lemma 7. *V, x_1, ϵ, η, u, $x_2, \ldots, x_n$, and $\hat{x}_2, \ldots, \hat{x}_n$ go to 0 exponentially as $\tau \to \infty$.*

Proof. Noting from Lemma 6 that solutions to the closed-loop dynamical system exist over $[0, \infty)$ and noting from the dynamics of $\hat{\theta}$ and r that both $\hat{\theta}$ and r are monotonically nondecreasing with τ and go to ∞ as $\tau \to \infty$, it is seen that a finite positive constant τ_0 exists such that $\hat{\theta} \geq \theta^*$ and $r^b \geq \theta^*$ for all time $\tau \geq \tau_0$. Hence, from (60), it follows that for all $\tau \geq \tau_0$, the inequality $\frac{dV}{d\tau} \leq -\kappa V$ is satisfied. Hence, V goes to 0 exponentially as $\tau \to \infty$. From the definition of V from (29), it follows that x_1, $\sqrt{r}|\epsilon|$, and $\sqrt{r}|\eta|$ go to 0 exponentially as $\tau \to \infty$. Since, we know from Lemma 6 that r grows at most polynomially in τ, it follows that $|\epsilon|$ and $|\eta|$ go to 0 exponentially as $\tau \to \infty$. From the form of u in (16), this implies that u goes to 0 exponentially as $\tau \to \infty$. Since $x_2 = r\eta_2 - \zeta - r\epsilon_2$ and $x_i = r^{i-1}(\eta_i - \epsilon_i)$, $i = 3, \ldots, n$, it therefore follows from Lemma 6 and the design of the function ζ that the signals $x_2, \ldots, x_n$ all go to 0 exponentially as $\tau \to \infty$. From the definition of functions f_i in (10), Assumption 1, and the fact that the functions g_i can be chosen to be linear constant-coefficient combinations of the functions $\phi_{(2,3)}, \ldots, \phi_{(n-1,n)}$ as noted in Section 3.6, it is seen that $\lim_{x_1 \to 0} \frac{f_i(x_1)}{x_1} = \frac{g_i(0)}{\phi_{(1,2)}(0)}$. Therefore, since x_1 goes to 0 exponentially as $\tau \to \infty$ while r grows at most polynomially, it is seen that $r^{i-1}f_i(x_1)$ goes to 0 exponentially as $\tau \to \infty$ for $i = 2, \ldots, n$. In addition, from the definition of the function ζ in (15) and noting that $\hat{\theta}$ grows at most polynomially, it follows that $\zeta(x_1, \hat{\theta})$ goes to 0 exponentially as $\tau \to \infty$. Hence, from the definition of $\eta_2, \ldots, \eta_n$ in (13) and (14), it is seen that the observer state signals $\hat{x}_2, \ldots, \hat{x}_n$ also go to 0 exponentially as $\tau \to \infty$. Hence, from the above analysis, we see that $V, x_1, \epsilon, \eta, u, x_2, \ldots, x_n$, and $\hat{x}_2, \ldots, \hat{x}_n$ all go to 0 exponentially as $\tau \to \infty$. ◇ ∎

Conclusion of the proof of Theorem 1: Since $\tau \to \infty$ corresponds to $t \to T$, the properties in Lemma 7 hold as $t \to T$. Therefore, the signals x, u, and $\hat{x} = [\hat{x}_2, \ldots, \hat{x}_n]^T$ all go to 0 as $t \to T$, that is, prescribed-time stabilization is attained. Note that $T > 0$ can be arbitrarily picked by the control designer; given any $T > 0$, the control design procedure developed in this article enables prescribed-time stabilization with convergence as $t \to T$. ◇

Remark 6. As discussed above, the control design ensures that x and u go to 0 as $t \to T$, that is, as $\tau \to \infty$. In addition, the observer state variables $\hat{x}_2, \ldots, \hat{x}_n$, the vector of scaled observer errors ϵ, and the vector of scaled observer estimates η all go to 0 as $t \to T$. However, the *control gains*, which from (16) involve r^n, go to ∞ as $t \to T$. The characteristic that control gains go to ∞ as t approaches the desired prescribed time T is intrinsic to the prescribed-time stabilization problem and is shared with previous results in prescribed-time stabilization.[26,27,33] It has been noted in References 26,27,33 that indeed *any* approach for regulation in finite time (including optimal control with a terminal constraint and sliding mode control based approaches with time-varying gains) will share this characteristic. Nevertheless, by the analysis above, we see that the unbounded gains do not result in an unbounded control input u (which indeed converges to 0). However, an implementation challenge can be posed by the fact that r goes to ∞ as $\tau \to \infty$. As shown in References 38,45, this numerical challenge in implementing the dynamics of r can be alleviated through a temporal scaling $\tilde{r} = rz$ where $z : \mathcal{R} \to \mathcal{R}$ is a function of τ and computing r via the scaled state variable $\tilde{r}$ instead of implementing the dynamics of r directly. By picking, for example, $z(\tau) = e^{-k_z\tau}$ with $k_z > 0$ being any constant, it is seen that the scaled state variable $\tilde{r} = rz$ is uniformly bounded over the time interval $\tau \in [0, \infty)$ since we know from Lemma 6 from r grows at most polynomially in τ; furthermore, it is seen that $\tilde{r}$ goes to 0 asymptotically as $\tau \to \infty$. In addition, from the dynamics of r in (51), it is seen that all the terms appearing in the expression for $\dot{r} = \alpha(\tau)\frac{dr}{d\tau}$ grow at most polynomially in τ. Hence, it is seen that $\dot{\tilde{r}}$ is uniformly bounded and goes to zero as $\tau \to \infty$, that is, as $t \to \infty$. In addition, to alleviate numerical difficulties in implementation due to unbounded gains as $t \to T$ (specifically, the facts that $\alpha(\tau)$, r, and $\hat{\theta}$ go to ∞ as $t \to T$), a few approaches can be utilized as noted in Reference 27. These approaches include adding a dead zone on the state x, a saturation on control gains, and setting the terminal time in the controller implementation to be some $\overline{T} > T$. All of these approaches sacrifice asymptotic convergence of x to 0 as $t \to T$ (ie, x goes not to 0, but to a small neighborhood of 0 as $t \to T$), but facilitate practical implementation by preventing unbounded gains.[27] ◇

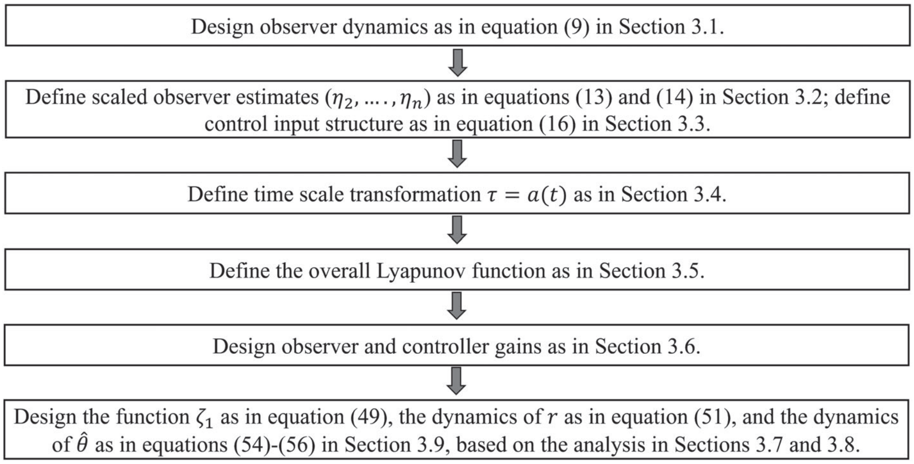

FIGURE 1 Block diagram of the overall design procedure for the proposed output-feedback prescribed-time stabilizing controller for the class of uncertain strict-feedback-like systems (1)

Remark 7. The designed controller is of dynamic order $(n+2)$ with the controller state comprising of the observer state variables $\hat{x}_2, \ldots, \hat{x}_n$, the dynamic scaling variable r, and the dynamic adaptation state variables $\hat{\theta}_1$ and $\hat{\theta}_2$. The overall controller is given by the observer dynamics (9), the definition of scaled states $\eta_2, \ldots, \eta_n$ in (14), the control law for u in (16), the choice of ζ and ζ_1 in (15) and (49), the dynamics of the adaptation parameters $\hat{\theta}_1$ and $\hat{\theta}_2$ in (55) and (56), and the dynamics of scaling parameter r in (51). The overall design procedure is shown in Figure 1.

5 | AN ILLUSTRATIVE EXAMPLE

Consider the third-order system

$$\begin{aligned} \dot{x}_1 &= (1 + x_1^2)x_2 \quad ; \quad y = x_1, \\ \dot{x}_2 &= (1 + x_1^4)x_3 + \theta_a e^{x_1} x_2, \\ \dot{x}_3 &= u + \theta_b x_1^5 x_3 + \theta_c x_1^2 \cos(x_3) x_2, \end{aligned} \tag{68}$$

where θ_a, θ_b, and θ_c are uncertain parameters (with no magnitude bounds required to be known). Only the output $y = x_1$ is assumed to be measured. It can be seen that the uncertain parameters appear multiplied with unmeasured state variables x_2 and x_3. Here, $\phi_{(1,2)}(x_1) = 1 + x_1^2$, $\phi_{(2,3)}(x_1) = 1 + x_1^4$, and $\mu_0(x_1) = 1$. This system satisfies Assumption 1 with $\sigma = 1$. Assumption 2 is satisfied with $\phi_{(1,1)} = \phi_{(2,1)} = \phi_{(3,1)} = 0$, $\phi_{(2,2)} = 1$, $\phi_{(3,2)} = |x_1|$, $\phi_{(3,3)} = x_1^4$, $\theta = \max\{\bar{c}_\theta \theta_a, \bar{c}_\theta \theta_b, \bar{c}_\theta \theta_c\}$ with $\bar{c}_\theta$ being any positive constant, and $\Gamma(x_1) = \frac{1}{\bar{c}_\theta}(|x_1| + e^{x_1})$. Note that the form of the terms $\theta_a e^{x_1} x_2$ and $\theta_b x_1^5 x_3 + \theta_c x_1^2 \cos(x_3) x_2$ in the dynamics are not required to be known as long as bounds as in Assumption 2 are known. Assumption 3 is trivially satisfied since $n = 3$.

Using the constructive procedure in References 39,47,48, a symmetric positive-definite matrix P_c and functions k_2 and k_3 can be found to satisfy the coupled Lyapunov inequalities (31) as $P_c = \tilde{a}_c \begin{bmatrix} 3 & 1 \\ 1 & 1 \end{bmatrix}$, $k_2 = 5\phi_{(2,3)}$, and $k_3 = 4\phi_{(2,3)}$, and with $\nu_c = 1.675\tilde{a}_c$, $\underline{\nu}_c = \tilde{a}_c$, and $\overline{\nu}_c = 5\tilde{a}_c$ with $\tilde{a}_c$ being any positive constant. In addition, using the constructive procedure in References 39,47,48, a symmetric positive-definite matrix P_o and functions g_2 and g_3 can be found to satisfy the coupled Lyapunov inequalities (32) as $P_o = \tilde{a}_o \begin{bmatrix} 30 & -5 \\ -5 & 2.5 \end{bmatrix}$, $g_2 = 12\phi_{(2,3)}$, and $g_3 = 20\phi_{(2,3)}$, and with $\nu_o = 6.675\tilde{a}_o$, $\tilde{\nu}_o = 32.070\tilde{a}_o$, $\underline{\nu}_o = 3.698\tilde{a}_o$, and $\overline{\nu}_o = 33.802\tilde{a}_o$ with $\tilde{a}_o$ being any positive constant. The inequality (33) is satisfied with $\overline{G} = 23.324$. As in Section 3, the functions f_2 and f_3 are defined as $f_2(x_1) = 12\int_0^{x_1} \frac{(1+x_1^4)}{1+x_1^2} d\pi$ and $f_3(x_1) = 20\int_0^{x_1} \frac{(1+x_1^4)}{1+x_1^2} d\pi$. These integrals in the definitions of the functions $f_2(x_1)$ and $f_3(x_1)$ can be evaluated in closed form using $\int_0^{x_1} \frac{(1+x_1^4)}{1+x_1^2} d\pi = \frac{x_1^3}{3} - x_1 + 2\tan^{-1}(x_1)$. A reduced-order observer is designed as

$$\dot{\hat{x}}_2 = (1 + x_1^4)[\hat{x}_3 + r^2 f_3(x_1)] - r g_2(x_1)[\hat{x}_2 + r f_2(x_1)] - \dot{r} f_2(x_1), \tag{69}$$

$$\dot{\hat{x}}_3 = u - r^2 g_3(x_1)[\hat{x}_2 + r f_2(x_1)] - 2\dot{r} r f_3(x_1). \tag{70}$$

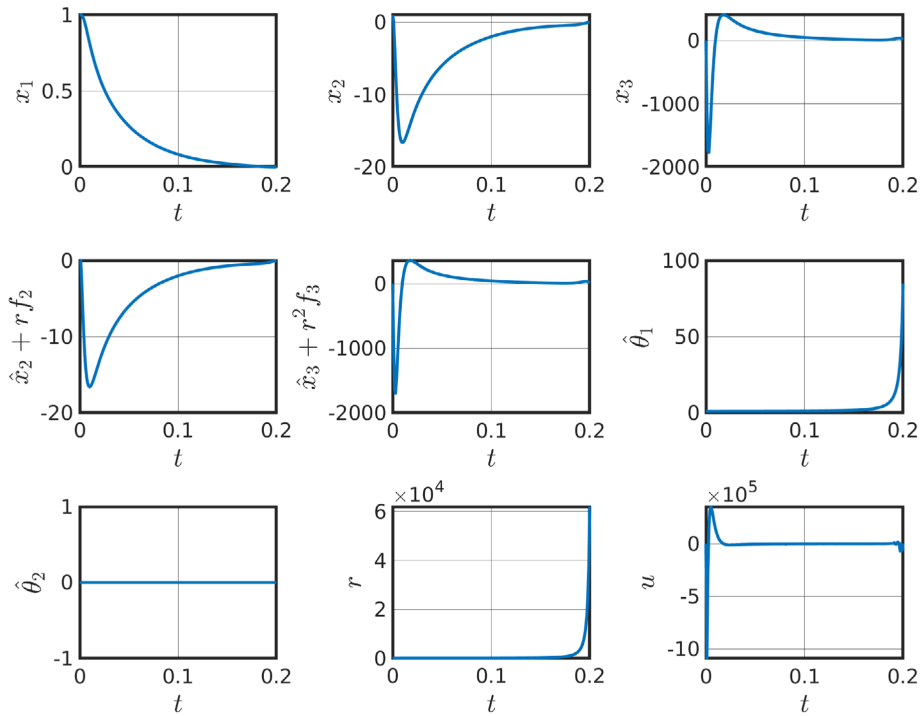

FIGURE 2 Simulations for the closed-loop system (system (68) in closed loop with the prescribed-time stabilizing adaptive output-feedback controller) [Colour figure can be viewed at wileyonlinelibrary.com]

Then, defining $\eta_2 = \frac{\hat{x}_2 + r f_2(x_1) + \zeta(x_1, \hat{\theta})}{r}$ and $\eta_3 = \frac{\hat{x}_3 + r^2 f_3(x_1)}{r^2}$, the control input is designed as $u = -r^3[k_2\eta_2 + k_3\eta_3]$. The function α is picked for instance as in (26) in Remark 4 with any $a_0 > 0$. The function q_1 is given in (45). The function q_2 reduces to 0 for this system since $\phi_{(1,1)} = 0$. The function ζ_1 is then defined as in (49) and the function ζ is defined as in (15). The functions w_1 and w_2 can be computed following the procedure in Section 3 (which yielded Equations (47) and (48)) using sharper bounds taking the specific system structure into account and noting that several terms in the upper bounds vanish since $\phi_{(1,1)}$, and so on, are zero for this system. Finally, the function Ω is defined as in (53) and the dynamics of r is defined as in (51). The dynamic adaptation parameter $\hat{\theta}$ is defined as the combination $\hat{\theta}_1 + \hat{\theta}_2$ as in (54) and the dynamics of $\hat{\theta}_1$ and $\hat{\theta}_2$ are defined as in (55) and (56).

Taking the unknown values of θ_a, θ_b, and θ_c to be $\theta_a = \theta_b = \theta_c = 2$, the numerical simulation of the closed-loop system is shown in Figure 2 with initial conditions for the system state vector $[x_1, x_2, x_3]^T$ being $[1, 1, 1]^T$. Since the initial conditions for x_2 and x_3 are not known, the initial conditions for $\hat{x}_2$ and $\hat{x}_3$ are picked simply as the values that make the initial values of the estimates for x_2 and x_3 zero, that is, such that $\hat{x}_2 + r f_2(x_1)$ and $\hat{x}_3 + r^2 f_3(x_1)$ are zero at time $t = 0$. Hence, the initial condition for $[\hat{x}_2, \hat{x}_3]^T$ is $[-10.85, -18.08]^T$. The initial conditions for r, $\hat{\theta}_1$, and $\hat{\theta}_2$ are picked to be 1, 1, and 0, respectively. Note that for this system, $\frac{d\hat{\theta}_2}{d\tau}$ reduces to 0 since as seen from (56), $\frac{d\hat{\theta}_2}{d\tau}$ has $q_2(x_1)$ as a factor and $q_2(x_1)$ is found to be 0 for this example system as noted above. Therefore, with $\hat{\theta}_2$ initialized to be 0, it is identically 0 for all time. The terminal time for prescribed-time stabilization is specified as $T = 0.2$ s. To avoid numerical issues, the effective terminal time $\overline{T}$ in implementation is defined as $\overline{T} = 0.205$ s. The constant c_0 in the dynamics of r in (51) is given by (52) and the constants c_1 and b are picked as 0.1 and 0.02, respectively. In addition, $a_0 = 0.05$, $\tilde{a}_c = 0.1$, $\tilde{a}_o = 0.5$, $\zeta_0 = 0.1$, $c_\theta = 10^{-3}$, and $\overline{c}_\theta = 10^5$. The closed-loop trajectories and the control input signal are shown in Figure 2.

6 | CONCLUSION

An adaptive dynamic output-feedback prescribed-time stabilizing controller was developed for a general class of uncertain nonlinear strict-feedback-like systems which allows uncertain functions that can include crossproducts of unknown parameters (without requiring any known magnitude bounds on the uncertain parameters) and unmeasured state variables. The design introduced several novel ingredients based on designs of time-varying dynamics of an adaptation state variable and the high-gain scaling parameter to ensure that the uncertain parameters (without any known magnitude bounds) that are coupled with the unmeasured state variables are dominated by the adaptation state variable and a fractional power of the dynamic high-gain scaling parameter within a subinterval of the prescribed time interval so as to achieve exponential state and input convergence to zero within the remaining subinterval of the prescribed time interval. The control design is performed over a transformed temporal representation that maps the finite prescribed time interval to an infinite interval in the transformed time axis. It was shown that given any desired convergence time, the proposed adaptive output-feedback control design provides both prescribed-time state estimation and prescribed-time state regulation for the considered class of uncertain nonlinear systems irrespective of the initial conditions. It is a topic of on-going work to determine if the proposed approach can be extended to other general classes of nonlinear systems (eg, feedforward and nontriangular systems and systems with delays, appended dynamics, or input unmodeled dynamics).

DATA AVAILABILITY STATEMENT

Data sharing not applicable since the article describes theoretical research.

ORCID

Farshad Khorrami https://orcid.org/0000-0002-8418-004X

REFERENCES

1. Krishnamurthy P, Khorrami F, Krstic M. Adaptive output-feedback prescribed-time stabilization of uncertain nonlinear strict-feedback-like systems. Paper presented at: Proceedings of the 2019 IEEE 58th Conference on Decision and Control (CDC); 2019:4240-4245; Nice, France.
2. Krstić M, Kanellakopoulos I, Kokotović PV. *Nonlinear and Adaptive Control Design*. New York, NY: Wiley; 1995.
3. Jain S, Khorrami F. Robust adaptive control of a class of nonlinear systems: state and output feedback. Paper presented at: Proceedings of 1995 American Control Conference-ACC'95 1995 Jun 21; 1995:1580-1584; IEEE, Seattle, WA.
4. Isidori A. *Nonlinear Control Systems*. Vol II. London, UK: Springer; 1999.
5. Khalil H. *Nonlinear Systems*. Prentice Hall: Upper Saddle River, NJ; 2001.
6. Haimo VT. Finite time controllers. *SIAM J Control Optim*. 1986;24(4):760-770.
7. Bhat SP, Bernstein DS. Finite-time stability of continuous autonomous systems. *SIAM J Control Optim*. 2000;38(3):751-766.
8. Huang X, Lin W, Yang B. Global finite-time stabilization of a class of uncertain nonlinear systems. *Automatica*. 2005;41(5):881-888.
9. Hong Y, Jiang ZP. Finite-time stabilization of nonlinear systems with parametric and dynamic uncertainties. *IEEE Trans Automat Control*. 2006;51(12):1950-1956.
10. Seo S., Shim H., Seo J. H.. Global finite-time stabilization of a nonlinear system using dynamic exponent scaling. 2008 47th IEEE Conference on Decision and Control 2008; December 9; 2008:3805-3810; IEEE; Cancun, Mexico.
11. Moulay E, Perruquetti W. Finite time stability conditions for non-autonomous continuous systems. *Int J Control*. 2008;81:797-803.
12. Shen Y, Huang Y. Global finite-time stabilisation for a class of nonlinear systems. *Int J Syst Sci*. 2012;43(1):73-78.
13. Polyakov A, Efimov D, Perruquetti W. Finite-time and fixed-time stabilization: Implicit Lyapunov function approach. *Automatica*. 2015;51(1):332-340.
14. Sun ZY, Xue LR, Zhang KM. A new approach to finite-time adaptive stabilization of high-order uncertain nonlinear system. *Automatica*. 2015;58:60-66.
15. Sun Z-Y, Yun M-M, Li T. A new approach to fast global finite-time stabilization of high-order nonlinear system. *Automatica*. 2017;81:455-463.
16. Andrieu V, Praly L, Astolfi A. Homogeneous approximation, recursive observer design, and output feedback. *SIAM J Control Optim*. 2008;47(4):1814-1850.
17. Wang H, Zhu Q. Finite-time stabilization of high-order stochastic nonlinear systems in strict-feedback form. *Automatica*. 2015;54:284-291.
18. Sun Z-Y, Shao Y, Chen C-C. Fast finite-time stability and its application in adaptive control of high-order nonlinear system. *Automatica*. 2019;106:339-348.
19. Sun Z-Y, Dong Y-Y, Chen C-C. Global fast finite-time partial state feedback stabilization of high-order nonlinear systems with dynamic uncertainties. *Inf Sci*. 2019;484:219-236.
20. Sun Z-Y, Zhou C-Q, Chen C-C, Meng Q. Fast finite-time adaptive stabilization of high-order uncertain nonlinear systems with output constraint and zero dynamics. *Inf Sci*. 2020;514:571-586.
21. Polyakov A. Nonlinear feedback design for fixed-time stabilization of linear control systems. *IEEE Trans Automat Control*. 2012;57(8):2106-2110.
22. Polyakov A, Efimov D, Perruquetti W. Robust stabilization of MIMO systems in finite/fixed time. *Int J Robust Nonlinear Control*. 2016;26(1):69-90.
23. Zimenko K, Polyakov A, Efimov D, Perruquetti W. Finite-time and fixed-time stabilization for integrator chain of arbitrary order. Paper presented at: Proceedings of the 2018 European Control Conference (ECC); 2018:1631-1635; IEEE, Limassol, Cyprus.
24. Zimenko K, Polyakov A, Efimov D, Perruquetti W. On simple scheme of finite/fixed-time control design. *Int J Control*. 2020;93(6):1353–1361.
25. Aldana-López R, Gómez-Gutiérrez D, Jiménez-Rodríguez E, Sánchez-Torres JD, Defoort M. Enhancing the settling time estimation of a class of fixed-time stable systems. *Int J Robust Nonlinear Control*. 2019;29(12):4135-4148.

26. Song Y, Wang Y, Holloway J, Krstic M. Time-varying feedback for finite-time robust regulation of normal-form nonlinear systems. Paper presented at: Proceedings of the 2016 IEEE 55th Conference on Decision and Control (CDC) 2016 December 12; 2016:3837-3842; IEEE; Las Vegas, NV.
27. Song Y, Wang Y, Holloway J, Krstic M. Time-varying feedback for regulation of normal-form nonlinear systems in prescribed finite time. *Automatica*. 2017;83:243-251.
28. Jiménez-Rodríguez E, Sánchez-Torres JD, Gómez-Gutiérrez D, Loukianov AG. Predefined-time stabilization of high order systems. Paper presented at: Proceedings of the 2017 American Control Conference (ACC); 2017:5836-5841; IEEE, Seattle, WA.
29. Jiménez-Rodríguez E, Sánchez-Torres JD, Loukianov AG. On optimal predefined-time stabilization. *Int J Robust Nonlinear Control*. 2017;27(17):3620-3642.
30. Tran D, Yucelen T, Sarsilmaz B. Control of multiagent networks as systems: finite-time algorithms, time transformation, and separation principle. Paper presented at: Proceedings of the 2018 IEEE Conference on Decision and Control (CDC); 2018:6204-6209; IEEE, Miami Beach, FL.
31. Becerra HM, Vázquez CR, Arechavaleta G, Delfin J. Predefined-time convergence control for high-order integrator systems using time base generators. *IEEE Trans Control Syst Technol*. 2018;26(5):1866-1873.
32. Sánchez-Torres JD, Gómez-Gutiérrez D, López E, Loukianov AG. A class of predefined-time stable dynamical systems. *IMA J Math Control nf*. 2018;35(Suppl 1):i1-i29.
33. Song Y, Wang Y, Krstic M. Time-varying feedback for stabilization in prescribed finite time. *Int J Robust Nonlinear Control*. 2019;29(3):618-633.
34. Sánchez-Torres JD, Defoort M, Muñoz-Vázquez AJ. Predefined-time stabilisation of a class of nonholonomic systems. *Int J Control*. 2019. https://www.tandfonline.com/doi/abs/10.1080/00207179.2019.1569262?journalCode=tcon20.
35. Zhao K, Song Y, Wang Y. Regular error feedback based adaptive practical prescribed time tracking control of normal-form nonaffine systems. *J Frankl Inst*. 2019;356(5):2759-2779.
36. Rekasius Z. An alternate approach to the fixed terminal point regulator problem. *IEEE Trans Automat Control*. 1964;9(3):290-292.
37. Morasso P, Sanguineti V, Spada G. A computational theory of targeting movements based on force fields and topology representing networks. *Neurocomputing*. 1997;15(3-4):411-434.
38. Krishnamurthy P, Khorrami F, Krstic M. Prescribed-time stabilization of nonlinear strict-feedback-like systems. Paper presented at: Proceedings of the 2019 American Control Conference (ACC) ; 2019:3081-3086; IEEE, Philadelphia, PA.
39. Krishnamurthy P, Khorrami F. Dynamic high-gain scaling: state and output feedback with application to systems with ISS appended dynamics driven by all states. *IEEE Trans Automat Control*. 2004;49(12):2219-2239.
40. Krishnamurthy P, Khorrami F. A high-gain scaling technique for adaptive output feedback control of feedforward systems. *IEEE Trans Automat Control*. 2004;49(12):2286-2292.
41. Krishnamurthy P, Khorrami F. Feedforward systems with ISS appended dynamics: adaptive output-feedback stabilization and disturbance attenuation. *IEEE Trans Automat Control*. 2008;53(1):405-412.
42. Krishnamurthy P, Khorrami F. High-gain output-feedback control for nonlinear systems based on multiple time scaling. *Syst Control Lett*. 2007;56(1):7-15.
43. Krishnamurthy P, Khorrami F. Generalized state scaling and applications to feedback, feedforward, and non-triangular nonlinear systems. *IEEE Trans Automat Control*. 2007;52(1):102-108.
44. Krishnamurthy P, Khorrami F. A singular perturbation based global dynamic high gain scaling control design for systems with nonlinear input uncertainties. *IEEE Trans Automat Control*. 2013;58(10):2686-2692.
45. Krishnamurthy P, Khorrami F, Krstic M. Robust output-feedback prescribed-time stabilization of a class of nonlinear strict-feedback-like systems. Paper presented at: Proceedings of the 2019 18th European Control Conference (ECC); 2019:1148-1153; IEEE, Naples, Italy.
46. Krishnamurthy P, Khorrami F. Dual high-gain-based adaptive output-feedback control for a class of nonlinear systems. *Int J Adapt Control Signal Process*. 2008;22(1):23-42.
47. Krishnamurthy P, Khorrami F. Conditions for uniform solvability of parameter-dependent Lyapunov equations with applications. Paper presented at: Proceedings of the 2004 American Control Conference; 2004:3896-3901; IEEE; Boston, MA.
48. Krishnamurthy P, Khorrami F. On uniform solvability of parameter-dependent Lyapunov inequalities and applications to various problems. *SIAM J Control Optim*. 2006;45(4):1147-1164.

How to cite this article: Krishnamurthy P, Khorrami F, Krstic M. Adaptive output-feedback stabilization in prescribed time for nonlinear systems with unknown parameters coupled with unmeasured states. *Int J Adapt Control Signal Process*. 2020;1–19. https://doi.org/10.1002/acs.3193